Aging influence on pulmonary and systemic inflammation and neural metabolomics arising from pulmonary multi-walled carbon nanotube exposure in apolipoprotein E-deficient and C57BL/6 female mice

Tamara L. Young, David Scieszka, Jessica G. Begay, Selita N. Lucas, Guy Herbert, Katherine Zychowski, Russell Hunter, Raul Salazar, Andrew K. Ottens, Aaron Erdely, Haiwei Gu & Matthew J. Campen

Taylor & Francis
Taylor & Francis Group

Check for updates

RESEARCH ARTICLE

Aging influence on pulmonary and systemic inflammation and neural metabolomics arising from pulmonary multi-walled carbon nanotube exposure in apolipoprotein E-deficient and C57BL/6 female mice

Tamara L. Young[a], David Scieszka[a], Jessica G. Begay[a], Selita N. Lucas[a], Guy Herbert[a], Katherine Zychowski[b] (iD), Russell Hunter[a], Raul Salazar[a], Andrew K. Ottens[c], Aaron Erdely[d], Haiwei Gu[e,f] and Matthew J. Campen[a] (iD)

[a]Department of Pharmaceutical Sciences, University of New Mexico, Albuquerque, NM, USA; [b]College of Nursing, University of New Mexico, Albuquerque, NM, USA; [c]Department of Anatomy and Neurobiology, Virginia Commonwealth University, Richmond, VA, USA; [d]Pathology and Physiology Research Branch, National Institute for Occupational Safety and Health, Morgantown, WV, USA; [e]College of Health Solutions, Arizona State University, Phoenix, AZ, USA; [f]Center for Translational Science, Florida International University, Port St. Lucie, FL, USA

ABSTRACT

Objective: Environmental exposures exacerbate age-related pathologies, such as cardiovascular and neurodegenerative diseases. Nanoparticulates, and specifically carbon nanomaterials, are a fast-growing contributor to the category of inhalable pollutants, whose risks to health are only now being unraveled. The current study assessed the exacerbating effect of age on multiwalled-carbon nanotube (MWCNT) exposure in young and old C57BL/6 and ApoE$^{-/-}$ mice.

Materials and methods: Female C57BL/6 and apolipoprotein E-deficient (ApoE$^{-/-}$) mice, aged 8 weeks and 15 months, were exposed to 0 or 40 μg MWCNT via oropharyngeal aspiration. Pulmonary inflammation, inflammatory bioactivity of serum, and neurometabolic changes were assessed at 24 h post-exposure.

Results: Pulmonary neutrophil infiltration was induced by MWCNT in bronchoalveolar lavage fluid in both C57BL/6 and ApoE$^{-/-}$. Macrophage counts decreased with MWCNT exposure in ApoE$^{-/-}$ mice but were unaffected by exposure in C57BL/6 mice. Older mice appeared to have greater MWCNT-induced total protein in lavage fluid. BALF cytokines and chemokines were elevated with MWCNT exposure, but CCL2, CXCL1, and CXCL10 showed reduced responses to MWCNT in older mice. However, no significant serum inflammatory bioactivity was detected. Cerebellar metabolic changes in response to MWCNT were modest, but age and strain significantly influenced metabolite profiles assessed. ApoE$^{-/-}$ mice and older mice exhibited less robust metabolite changes in response to exposure, suggesting a reduced health reserve.

Conclusions: Age influences the pulmonary and neurological responses to short-term MWCNT exposure. However, with only the model of moderate aging (15 months) in this study, the responses appeared modest compared to inhaled toxicant impacts in more advanced aging models.

Introduction

Aging is an ongoing degenerative process resulting from complex interactions between genetics and various environmental factors. Aging produces physiological and pathological changes, including reduced energy production and utilization, impaired molecular/cellular/tissue repair mechanisms, neuropathology, and increased inflammation from the accumulation of senescent cells (Bratic and Larsson 2013; Wagner et al. 2016; Bektas et al. 2018; Smith and Bhatnagar 2018). As a result, aging is the strongest risk factor for many pathologies, including cardiovascular, metabolic, and neurological diseases. Epidemiological studies on the public health impact of air pollution provide strong evidence for negative effects on aging-related diseases and further indicate that individuals of advanced age may be vulnerable to toxic outcomes.

Particulate matter (PM) inhalation (environmental and engineered) as an environmental driver of aging-related diseases has broad global health implications. The World Health Organization estimates that 9 out of 10 persons globally are exposed daily to PM-polluted air that surpasses their set limits, resulting in 7 million people worldwide dying prematurely every year (World Health Organization 2018). The full impact of aging on responses to inhaled pollutants is currently incompletely characterized, although studies have shown that long-term exposure to ambient air pollution significantly reduces life expectancy and exacerbates age-related diseases in human populations (Pope et al. 2009; Brook et al. 2010). Air pollution exposure is significantly associated with increased adverse cardiovascular outcomes, with sustained exposure to PM promoting increased mortality resulting from ischemic heart disease, arrhythmias,

and heart failure (Pope et al. 2004). Exposure to PM decreased blood oxygen levels in older male subjects (>80 years old) and accelerated pulse rate in all subjects, suggesting that advancing age compromises our ability to adequately respond to environmental stressors (Dockery et al. 1999). Furthermore, reducing PM in ambient air by $10\,\mu g/m^3$ is associated with an increase in life expectancy of approximately 0.77 years (Pope et al. 2009).

Neurological impacts of PM have largely focused on the role these exposures play in the development of Alzheimer's disease and related dementia. Grande et al. demonstrated that long-term exposure to air pollutants led to associations between heart failure, ischemic heart disease, and increased risk of dementia (Grande et al. 2020). Neuroinflammation is a hallmark of Alzheimer's and associated dementia (Heneka et al. 2015; Leng and Edison 2021) and so environmental stressors that promote either microglial activation or infiltration of peripheral leukocytes into the brain may exacerbate aging and related dementias. Tyler et al. showed that ozone exposure induced neuroinflammation, which could be significantly augmented in aging models, possibly as a result of blood–brain barrier deficits (Tyler et al. 2018). The consequences of engineered nanomaterials (ENM) on both pulmonary and systemic health are a more recent focus. We previously showed that short-term pulmonary exposure to multiwalled carbon nanotubes (MWCNT) led not only to pulmonary inflammation but to disruption in blood–brain barrier integrity and activation of astrocytes, as well as recruitment of microglia to areas of albumin leakage (Aragon et al. 2017). Very little data exists to inform our knowledge of the impact of aging in these exposures. In our human health effect studies of workers exposed to carbon nanotubes and nanofibers, age followed a bimodal distribution with 49% of the participants 45 years of age or older further supporting evaluations related to aging (Schubauer-Berigan et al. 2018).

Apolipoprotein E (ApoE), produced primarily in the liver, is also expressed in multiple lung cells (Yao et al. 2016; Kulminski et al. 2018) and in the central nervous system in astrocytes and microglia (to a lesser extent) (Mulder 2009; Achariyar et al. 2016). It has been shown to play an important role in maintaining pulmonary homeostasis and modulating responses to various inhalation exposures including immunoresponses. Additionally, the role of ApoE as a genetic risk factor for the pathogenesis of the aging-related neurodegenerative Alzheimer's disease is well explored (Liu et al. 2013; Yin and Wang 2018; Zhao et al. 2018). Altered pulmonary inflammatory responses to inhaled toxicants may be an important adaptation of aging and may influence the systemic and neural responses. Acute organic dust exposure in aged male C57BL/6 mice produced reduced inflammatory responses in the lung compared with young adult controls (Achariyar et al. 2016). Repeated exposures, however, led to increased inflammatory cell recruitment, suggesting that aging alters endogenous responses to particulate exposures and may impair the homeostatic benefits of inflammation (Poole et al. 2015). Reduced pulmonary inflammation in older animals was also observed following

inhaled ozone exposures; interestingly, however, neuroinflammation was increased (Mumaw et al. 2016), suggesting that acute pulmonary responses to air pollution exposure may be protective in reducing systemic toxicity.

In this study we assessed the impact of age on exposure to multiwalled carbon nanotubes (MWCNT), an engineered nanomaterial with well-studied pulmonary health effects, in young (2 months) and old (15 months) healthy and ApoE-deficient (ApoE$^{-/-}$) female mice. ApoE$^{-/-}$ mice exhibit elevated levels of circulating cholesterol that leads to vascular pathology (Zhang et al. 1992); humans exhibit an age-related increase in cholesterol that is also associated with vascular morbidity and mortality (He et al. 2021). MWCNT has been shown to induce consistent dose-dependent pulmonary inflammation and systemic toxicity following acute exposures (Aragon et al. 2017; Mostovenko et al. 2019). Neuroinflammatory activation observed following MWCNT exposure, in conjunction with serum peptide changes led us to examine the impact of these exposures on the initial pulmonary responses in a model of vascular disease with aging as a key component.

Methods

Animal model and sample collection

Specific pathogen-free female C57BL/6 and ApoE$^{-/-}$ mice (Jackson Laboratory) aged 6–8 weeks and 15 months were used in this study. Animals were housed in an Association for Assessment and Accreditation of Lab Animal Care International-approved animal facility at the University of New Mexico, with all experimental procedures approved by the Institutional Animal Care and Use Committee (IACUC) of the University of New Mexico. Animal care and use procedures were conducted in accordance with the US Public Health Service's Policy on Humane Care and Use of Laboratory Animals (https://grants.nih.gov/grants/olaw/references/phspol.htm) and the National Institutes of Health's Guide for the Care and Use of Laboratory Animals (https://grants.nih.gov/grants/olaw/Guide-for-the-Care-and-Use-of-Laboratory-Animals.pdf). Food and prepackaged water were provided *ad libitum* in ventilated cages in a temperature- and humidity-controlled environment with a 12-h light/dark cycle. Mice were administered MWCNT via oropharyngeal aspiration at doses of 0 μg or 40 μg ($n = 5$–7/group). The MWCNTs were prepared in a dispersion media (DM) consisting of mouse serum albumin (0.6 mg/ml) and 1,2-dipalmitoyl-sn-glycero-3-phosphocholine (10 μg/ml); DM was used as a control vehicle. The MWCNT material used in this study, Mitsui-7, has been extensively characterized (Porter et al. 2010; Erdely et al. 2013; Aragon, Erdely, et al. 2016; Fraser et al. 2020), with a mean diameter of 49 nm and length of 3.86 μm (geometric standard deviation = 1.94). Mice were euthanized 24-h following MWCNT pulmonary dosing. At the time of euthanasia, blood and bronchoalveolar lavage fluid (BALF) were collected. Serum was spun from the blood that was allowed to coagulate on ice for 30 min. Following transcardial perfusion with

ice-cold 1X PBS, the cerebellum was collected for metabolomic assessment.

Pulmonary inflammation assessment – mesoscale assay

MWCNT-induced changes in BALF cytokines were determined using the Meso Scale Discovery MULTI-SPOT V-PLEX® Cytokine Assay System Pro-inflammatory Panel 1 (mouse) Kits (K15048D - Meso Scale Diagnostics LLC, Rockville, MD) according to manufacturer's instructions. Briefly, BALF was collected by lavaging lungs of euthanized MWCNT exposed mice with ice-cold 1X PBS. Cell fractions were removed by centrifugation and 50 μl/well of the supernatant were loaded onto sample plates pre-coated with capture antibodies for the following cytokines: interferon-gamma (IFN-γ), interleukin-10 (IL-10), interleukin-12 (IL-12p70 active heterodimer), interleukin-1 beta (IL-1β), interleukin-2 (IL-2), interleukin-4 (IL-4), interleukin-5 (IL-5), interleukin-6 (IL-6), chemokine C-X-C motif ligand 1 (CXCL1, aka KC/GRO), and tumor necrosis factor-alpha (TNF-α). Plates were incubated with gentle shaking for 2 h at room temperature. Plates were washed 3X with buffer containing 1X PBS and 0.05% Tween 20. A detection antibody was added to each well and allowed to react for 1 h at room temperature. Plates were washed as above, and Read Buffer was added to each well. Plates were analyzed on an MSD QuickPlex SQ 120 instrument (MSD, AI0AA-0); Discovery Workbench (v. 4.0) software calculated cytokine concentrations using a linear regression analysis of the standard curve. All concentrations were normalized to total BALF protein, determined using a standard Bradford protein assay.

Serum cumulative inflammatory potential assay

Mouse cerebrovascular endothelial cells (mCEC) were obtained from a commercial vendor (Cell Biologics, Chicago, IL) and maintained according to manufacturer's recommendations at 37 °C and 5% CO$_2$ with complete endothelial cell medium supplemented with 5% fetal bovine serum. All experiments were conducted with cells between passages 3 and 8. To determine the serum cumulative inflammatory potential of MWCNT exposure, MBECs were treated with serum isolated from MWCNT-exposed and control mice as previously described (Cung et al. 2015; Zychowski et al. 2016). Briefly, MBECs were serum-starved overnight then incubated in FBS-free culture media supplemented at a final concentration of 5% v/v serum from control (0 μg) or 40 μg MWCNT exposed mice for 4 h and harvested. RNA was isolated using the RNeasy Mini Kit (QIAGEN, Germantown, MD), and reverse transcribed prior to gene expression analyses via quantitative real-time PCR (qPCR). Expression of mouse *Ccl2* (Mm00441242_m1), *Icam1* (Mm00516023_m1), *Il6* (Mm00446190-m1), *Tnfa* (Mm00443258_m1), *Tgfb* (Mm01178820_m1), and *Vcam1* (Mm01320970_m1) (Applied Biosystems, Foster City, CA) was measured using the TaqmanR Gene Expression protocol (ThermoScientific, Waltham, MA) following the

manufacturer's instructions. Relative gene expression normalized to the endogenous gene expression control TATA-Box Binding Protein (TBP) (Mm00446973_m1) gene was determined using the $2^{-\Delta\Delta CT}$ method for all samples with threshold cycle values (CT) under 35. Results are expressed as fold change.

Cerebellar metabolomics

Reagents

Acetonitrile (ACN), methanol (MeOH), ammonium acetate, and acetic acid, all liquid chromatography-tandem mass spectrometry (LC-MS/MS) grade, were purchased from Fisher Scientific (Pittsburgh, PA). Ammonium hydroxide was bought from Sigma-Aldrich (Saint Louis, MO). DI water was provided in-house by a Water Purification System from EMD Millipore (Billerica, MA). PBS was bought from GE Healthcare Life Sciences (Logan, UT). The standard compounds corresponding to the measured metabolites were purchased from Sigma-Aldrich (Saint Louis, MO) and Fisher Scientific (Pittsburgh, PA).

Tissue preparation

Briefly, each tissue sample ($\sim$20 mg; $n = 5$–6 per group) was homogenized in 200 μl MeOH:PBS (4:1, v:v, containing 1810.5 μM $^{13}C_3$-lactate and 142 μM $^{13}C_5$-glutamic Acid) in an Eppendorf tube using a Bullet Blender homogenizer (Next Advance, Averill Park, NY). Then 800 μl MeOH:PBS (4:1, v:v, containing 1810.5 μM $^{13}C_3$-lactate and 142 μM $^{13}C_5$-glutamic Acid) was added, and after vortexing for 10 s, the samples were stored at -20 °C for 30 min. The samples were then sonicated in an ice bath for 30 min, centrifuged at 14 000 RPM for 10 min (4 °C), and 800 μl supernatant was transferred to a new Eppendorf tube. The samples were then dried under vacuum using a CentriVap Concentrator (Labconco, Fort Scott, KS). Prior to MS analysis, the obtained residue was reconstituted in 150 μl 40% PBS/60% ACN. A quality control (QC) sample was pooled from all the study samples.

LC-MS/MS

The targeted LC-MS/MS method used here was modeled after that developed and used in a growing number of studies with detailed lists of metabolites (Carroll et al. 2015; Gu et al. 2015, 2016; Jasbi et al. 2019; Shi et al. 2019; Eghlimi et al. 2020). Briefly, we targeted $\sim$300 metabolites selected from >35 metabolic pathways of biological significance, including glycolysis, TCA cycle, purine metabolism, amino acid metabolism, etc. All LC-MS/MS experiments were performed on an Agilent 1290 UPLC-6490 QQQ-MS (Santa Clara, CA) system. Each sample was injected twice, 10 μl for analysis using negative ionization mode and 4 μl for analysis using positive ionization mode. Both chromatographic separations were performed using hydrophilic interaction chromatography (HILIC) on a Waters XBridge BEH Amide column (150 × 2.1 mm, 2.5 μm particle size, Waters Corporation, Milford, MA). The flow rate was 0.3 ml/min,

the auto-sampler temperature was kept at $4\,°C$, and the column compartment was set at $40\,°C$. The mobile phase was composed of Solvents A (10 mM ammonium acetate, 10 mM ammonium hydroxide in 95% H_2O/5% ACN) and B (10 mM ammonium acetate, 10 mM ammonium hydroxide in 95% ACN/5% H_2O). After the initial 1 min isocratic elution of 90% B, the percentage of Solvent B decreased to 40% at $t = 11$ min. The composition of Solvent B was maintained at 40% for 4 min ($t = 15$ min), and then the percentage of B gradually went back to 90%, to prepare for the next injection.

The mass spectrometer is equipped with an electrospray ionization (ESI) source. Targeted data acquisition was performed in multiple-reaction-monitoring (MRM) mode. All LC-MS/MS parameters, including MRM transitions, collision energy (CE), retention time, etc., were confirmed and validated using metabolite standards. The whole LC-MS system was controlled by Agilent Masshunter Workstation software (Santa Clara, CA). The extracted MRM peaks were integrated using Agilent MassHunter Quantitative Data Analysis (Santa Clara, CA).

Statistical analyses of metabolomics data RStudio

Packages used for dataset analyses and presentation: qqman for the Manhattan plot (https://github.com/drveera/ggman), dplyr for data transformation (https://cran.r-project.org/web/packages/dplyr/index.html), ggplot2 for graphing resultant plots (https://cran.r-project.org/web/packages/ggplot2/index.html), ggpubr for additional plotting of data (https://cran.r-project.org/web/packages/ggpubr/index.html), car for some statistical analysis and multi-way ANOVAs (https://cran.r-project.org/web/packages/car/index.html), foreign for read-write capabilities (https://cran.r-project.org/web/packages/foreign/index.html), rcompanion for graph alterations (https://cran.r-project.org/web/packages/rcompanion/index.html), and tidyverse for esthetic changes (https://cran.r-project.org/web/packages/tidyverse/index.html).

Targeted NAD + pathway analysis

After receiving the metabolomics data, we removed a single outlier mouse with a cerebellum weight of 7.8 g after performing a Grubb's test ($Z = 4.460$, $Z_{crit} = 3.10324$). The remaining metabolites were normalized per mouse weight. Linear discriminate analyses were performed for each mouse strain followed by multiway ANOVA ($p < 0.10$). To the statistically significant metabolites, Tukey's Honest Significant Differences tests were performed (confidence level $= 0.95$) to determine groupings.

Overall metabolite examination

The entire metabolite dataset was run recursively through three-way ANOVAs and a secondary database was generated from metabolites that showed statistical significance in at least one category of comparison. That dataset was used for the generation of the Manhattan plot (cutoff line at $1.3 = p < 0.05$, cutoff line at $2 = p < 0.01$.

Statistics

All statistics were conducted in GraphPad Prism (v9.0) or RStudio. Data were tested for Gaussian normality using a Shapiro-Wilk test; most data sets were observed to be normal. The infrequent nature of non-Gaussian distribution of data led to the choice of standard parametric statistical tests for all assays. Data were assessed as a two-way ANOVA, considering MWCNT and age as the 2 factors. Tukey's post-hoc multiple comparison test was used when appropriate. A three-way ANOVA was used for metabolomic data, considering MWCNT, age, and strain.

Results

Pulmonary inflammation

BALF inflammatory cell profile: C57BL/6 mice

Post-exposure assessment of BALF cell counts and total protein from MWCNT- and DM-exposed young and old mice revealed an age-independent inflammatory activation in C57BL/6 female mice (Figure 1). Total cell count and total protein were unchanged across age groups by MWCNT exposure (Figure 1(A,D)). Macrophage density was not significantly changed by MWCNT exposure (Figure 1(B)), although old animals display a lower trend in DM and MWCNT groups. The same MWCNT exposure led to a statistically significant increase in polymorphonuclear neutrophil (PMN) infiltration in both young and old animals ($p < 0.05$) (Figure 1(C)). The unchanged total cell and protein values may represent a shift in the inflammatory response resulting from macrophage-mediated increase in PMN infiltration in C57BL/6 animals.

BALF inflammatory cell profile: ApoE$^{-/-}$ mice

MWCNT exposure in the ApoE$^{-/-}$ model of impaired cholesterol clearance exhibited a greater overall inflammatory response as compared to C57BL/6 mice (Figure 2). ApoE$^{-/-}$ female mice showed no significant differences in the total cell count in response to MWCNT (Figure 2(A)) but exhibited a significant age-independent decrease in macrophage differential cell counts following MWCNT exposure ($p < 0.001$) (Figure 2(B)). The decreased macrophage cell count was accompanied by a statistically significant and robust BALF PMN increase following MWCNT exposure in both young and old animals ($p < 0.0001$; Figure 2(C)). The corresponding total protein assessment indicated an age-dependent BALF protein shift with older animals showing a significant increase in total protein in MWCNT-exposed groups compared with their DM controls (($p < 0.001$) and the MWCNT-exposed young counterparts ($p < 0.05$; Figure 2(D)).

The influence of age on total protein content after MWCNT treatment was statistically significant by two-way ANOVA analysis ($p < 0.05$), indicating an augmented response in older animals. Young ApoE$^{-/-}$ females did not show changes in total protein after MWCNT compared to young DM-treated mice, and the overall levels of protein were consistent with that measured in C57BL/6 mice. The responses to MWCNT exposure between C57BL/6 and
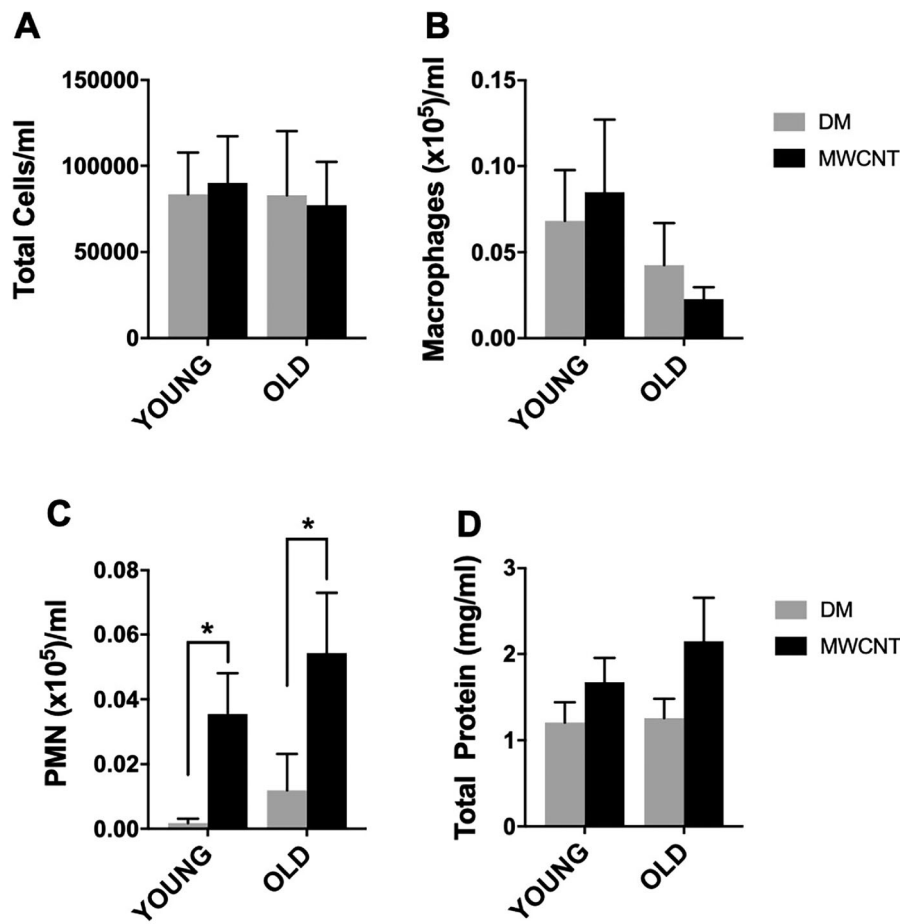
Figure 1. Airway inflammation in C57BL/6 female mice exposed to MWCNT. (A) Total cells in bronchoalveolar lavage (BALF); (B) macrophage differential cell counts; (C) polymorphonuclear leukocytes (PMN) differential cell counts; and (D) Total BALF protein. $n = 5–6$ per group. Data presented are means ± SEM. Asterisks (*) indicate significant effect of MWCNT by a 2-way ANOVA. No significant effect of age was noted.

ApoE$^{-/-}$ groups showed more robust responses in ApoE$^{-/-}$ mice, suggesting there may be an increased susceptibility to acute MWCNT exposure in this model compared to C57BL/6.

BALF cytokine expression: C57BL/6 mice

To further determine the level of inflammatory activation induced by MWCNT exposure, we assessed cytokine protein expression via Mesoscale ELISA assay. Differential exposure- and age-related cytokine profiles were revealed in both C57BL/6 and ApoE$^{-/-}$ groups. In C57BL/6 mice, MWCNT treatment and aging interactions were seen with major inflammatory cytokines IL-β, IL-6, and CCL2, with older mice exhibiting potentiated responses to MWCNT (Figure 3(A–C)). TNFα and MIP-1α were both significantly elevated by MWCNT treatment, but unaffected by age (Figure 3(D,E)). CXCL1 and CXCL10 both displayed significant induction due to MWCNT treatment that was attenuated in 15-mo mice (Figure 3(F,G)). Several cytokines remained unchanged by MWCNT and age (IFNγ, IL-10, IL-12p70; Figure 3(H–J)).

BALF cytokine expression: ApoE$^{-/-}$ mice

Unlike C57BL/6 mice, aging did not impact the magnitude of major inflammatory cytokines IL-β, IL-6, CCL2, and TNFα response to MWCNT in ApoE$^{-/-}$ (Figure 4(A–D)). 15-mo ApoE$^{-/-}$ mice did not exhibit a significant MIP-1α response

to MWCNT ($p = 0.09$), although younger ApoE$^{-/-}$ mice did (Figure 4(E)). Similar to findings in C57BL/6 mice, MWCNT treatment-induced CXCL1 and CXCL10 BALF increases were significantly greater in young mice compared to 15-mo mice (Figure 4(F,G)). Interestingly, MWCNT exposure produced a significant decrease in IFNγ BALF protein in 15-mo ApoE$^{-/-}$ mice (Figure 4(H)). IL-10 and IL-12p70 cytokines remained unchanged by either MWCNT and age (Figure 4(I,J)). In general, ApoE$^{-/-}$ mouse responses appeared dampened compared to C57BL/6. This was possibly a factor in limiting the lack of aging-associated augmentation of IL-β, IL-6, MCP-1, and TNFα responses to MWCNT.

A 3-way ANOVA was applied to compare the differences between C57BL/6 and ApoE$^{-/-}$ mice, along with age and MWCNT treatment. The 3-way ANOVA identified strain-dependent differences for MIP1a, CXCL10, IL1b, CXCL1, IL12p70, IL-10, and IFNγ. In all cases, the ApoE$^{-/-}$ mice appeared to have lower values at baseline or after response to MWCNT. Strain × MWCNT interactions were observed only for CXCL10 and IL-10.

Serum cumulative inflammatory potential assessment

To begin to define the systemic consequences of MWCNT exposure, we performed an *in vitro* assay using mCECs. mCECs were incubated with 5% serum from C57BL/6 and
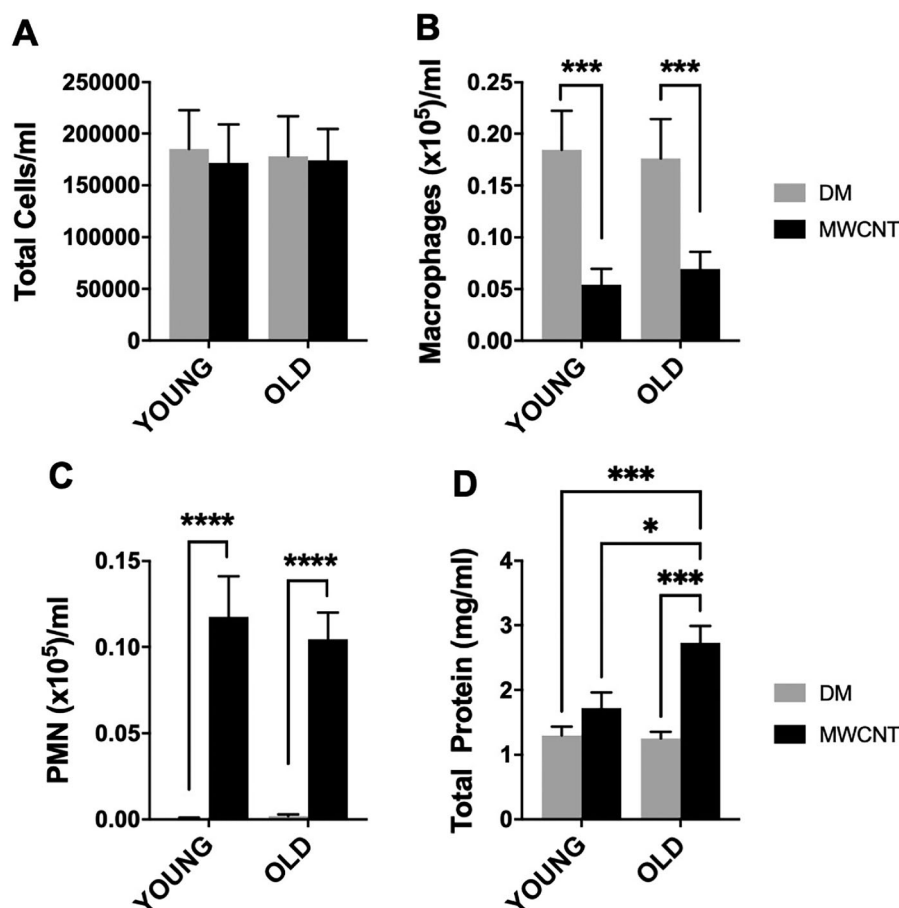
Figure 2. Airway inflammation in ApoE$^{-/-}$ female mice exposed to MWCNT. (A) Total cells in bronchoalveolar lavage (BALF); (B) Macrophage differential cell counts. Asterisks (***) indicate significant ($p < 0.001$) effect of MWCNT by a 2-way ANOVA. No significant effect of age was noted; (C) polymorphonuclear leuko-cytes (PMN) differential cell counts. Asterisks (****) indicate significant ($p < 0.0001$) effect of MWCNT by a 2-way ANOVA. No significant effect of age was noted; and (D) Total BALF protein. 2-way ANOVA revealed an interactive effect of age and MWCNT exposure, with old ApoE$^{-/-}$ mice displaying a significant increase in total protein compared to all other groups by Tukey's multiple comparison test (*$p < 0.05$; ***$p < 0.001$). $n = 5$–6 per group. Data presented are means ± SEM.

ApoE$^{-/-}$ animals to assess the degree of systemic bioactivity generated by lung MWCNT exposure and any age-related consequences (Figures 5 and 6). Using two-way ANOVAs, no effects were noted for MWCNT or age in each strain (C57BL/6 and ApoE$^{-/-}$). However, given that some of the trends were similar across the strains, we considered that our data may be underpowered and applied a three-way ANOVA to better incorporate all the data. Several significant trends emerged. Vcam1, for instance, was significantly upregulated in ApoE$^{-/-}$ mice ($p = 0.0084$) and we also saw an Age × Strain interaction ($p = 0.049$). A similar Strain related effect was seen for Tgfb ($p = 0.0106$) along with an interaction between Age × MWCNT treatment ($p = 0.0212$). A Strain effect was also seen for Icam1 ($p = 0.046$).

Neurometabolomics

To assess neurological consequences of MWCNT exposure in young and old mice, we assessed the metabolic changes in the cerebellum of exposed C57BL/6 and ApoE$^{-/-}$ animals (Figures 7–10). Complete heatmaps of metabolites for C57BL/6 and ApoE$^{-/-}$ mice are shown in Figure 7 (raw data provided in Supplemental Table 1). Linear discrimin-ation analyses found that C57BL/6 accuracy was estimated

at 80% by machine learning and 92% of the variance was explained in the dimensions shown (LD1 = 62.09%, LD2 = 29.67%, LD3 = 8.24%; Figure 8(A)). ApoE$^{-/-}$ data were subjected to the same analysis; however, the amount of colinear variables deemed the accuracy at 66% by machine learning, with 79% of variance explained in the first two dimensions (LD1 = 51.36%, LD2 = 28.55%, LD3 = 20.9%; Figure 8(B)). Analysis of C57BL/6 metabolomic responses produced more discrete grouping with MWCNT inducing a shift in young mice, but with little effect in old mice. APOE$^{-/-}$ animals showed more overlapping groupings between age and exposure, suggesting a muted overall metabolomic response. Further analyses are required to determine functional implications of the groups identified and the role the play in modulating cerebellar metabolic changes following MWCNT exposure.

A three-way analysis was conducted to examine the influ-ence of the major experimental factors (Age, Strain, MWCNT treatment) on cerebellar metabolites. A Manhattan plot (Figure 9) summarizes the outcomes, with the ApoE$^{-/-}$ strain having a major influence on metabolite concentrations in the cerebellum, with over 20 metabolites altered with $p < 0.01$. Age had a lesser effect with 7 metabo-lites different at $p < 0.01$ and 19 at $p < 0.05$ (no false
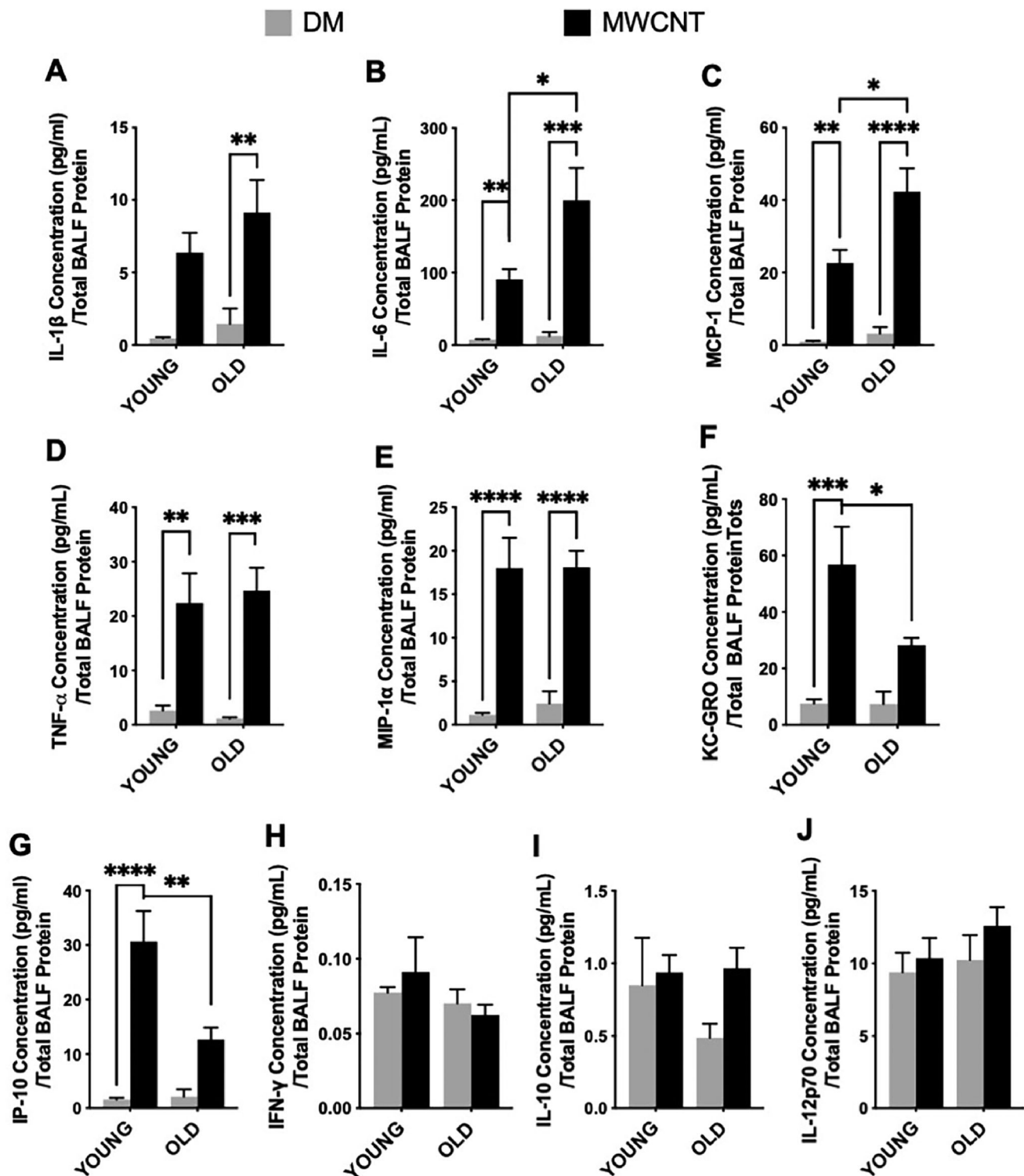
Figure 3. Airway cytokine expression in C57BL/6 female mice exposed to MWCNT. Cytokines are grouped according to pattern of response across dose and age. Some cytokines increased with MWCNT treatment and were augmented by advanced age, including IL-1b, IL-6, and MCP-1 [(A)–(C), respectively]. Some cytokines responded to MWCNT treatment and were unaffected by age, including TNFα and MIP-1α (D, E). Cytokines that were elevated by MWCNT in 2-mo mice but significantly reduced in 15-mo old mice included CXCL1 and CXCL10 (F, G). IFNγ, IL-10, and IL-12p70 were unchanged by MWCNT treatment or age. Asterisks indicate significant (*$p < 0.05$; **$p < 0.01$; ***$p < 0.001$; ****$p < 0.0001$) effect by a 2-way ANOVA with Tukey's multiple comparison test. $n = 5$–6 per group. Data presented are means ± SEM.

discovery rate correction applied). MWCNT exposure on its own induced minimal alterations (6 metabolites of $p < 0.05$), but interactions between age, strain, and MWCNT exposure identified several additional factors that may be altered by MWCNT only in older mice. A complete table of significantly altered metabolites, corresponding with the Manhattan plot is provided in the data supplement (Supplemental Table 2).
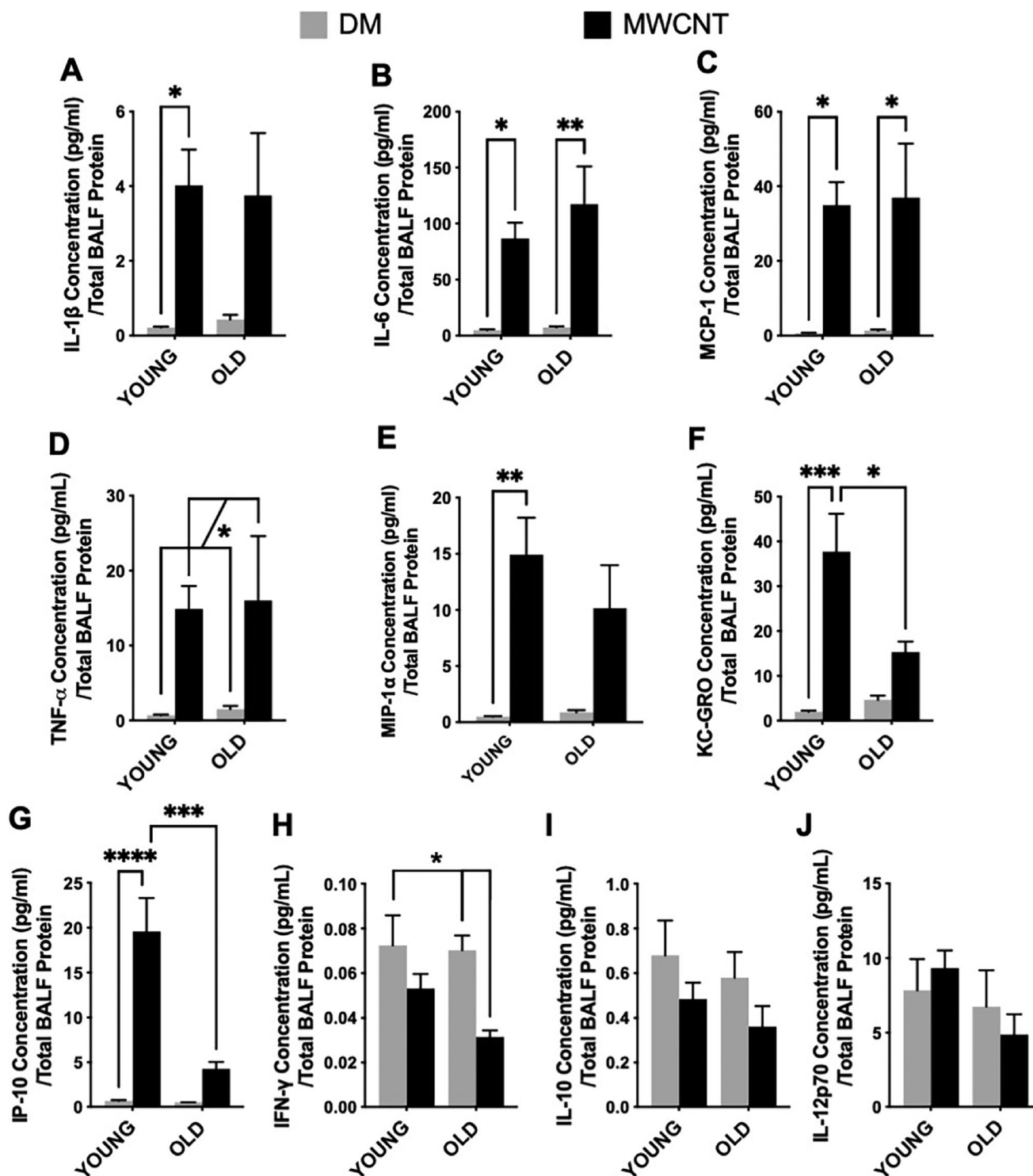
Figure 4. Airway cytokine expression in ApoE$^{-/-}$ female mice exposed to MWCNT. Cytokines are grouped according to pattern of response across dose and age. Some cytokines increased with MWCNT treatment but were unaffected by age, including IL-1β, IL-6, CCL2, TNFα, and MIP-1α [(A)–(E), respectively]. Cytokines that were elevated by MWCNT but significantly reduced in 15-mo old mice included CXCL1 and CXCL10 (F, G). 15-mo old mice treated with MWCNT displayed a significant reduction in IFNγ, and effect not seen in 2-mo old mice. IL-10 and IL-12p70 were unchanged by MWCNT treatment or age. Asterisks indicate significant (*$p < 0.05$; **$p < 0.01$; ***$p < 0.001$; ****$p < 0.0001$) effect by a 2-way ANOVA with Tukey's multiple comparison test. $n = 5$–6 per group. Data presented are means ± SEM.

Targeted nicotinamide adenine dinucleotide (NAD+) pathway analysis was performed to assess changes in cerebellar energetics and oxidative stress and the role played by age in mediating MWCNT effects (Figure 10). NAD$^+$ levels were significantly elevated by MWCNT exposure in young C57BL/6 animals but conversely decreased by exposure in young ApoE$^{-/-}$ animals. Old animals of either animal strain did not show significant changes with exposure to MWCNT. The precursor nicotinamide mononucleotide (NMN) was observed as statistically unchanged by exposure and age. Adenosine diphosphate (ADP) ribose was also investigated as a marker of MWCNT-induced DNA damage.
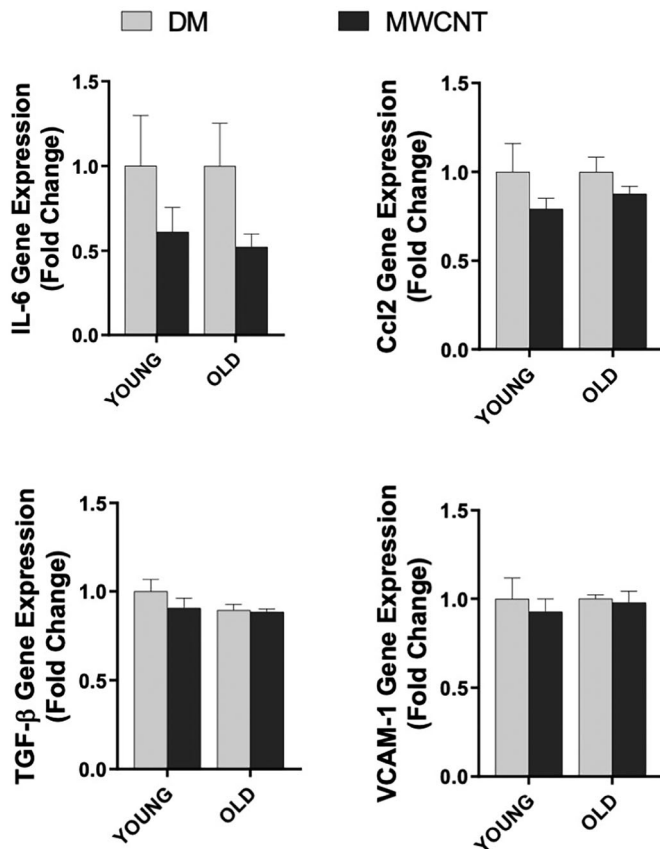
Figure 5. Serum Cumulative Inflammatory Potential (SCIP) assessment of serum from C57BL/6 female mice exposed to MWCNT. Mouse cerebrovascular endothelial cells (mCEC) were treated with serum from old and young dispersion media (DM; control) and MWCNT. Inflammatory gene expression changes were assessed via qPCR. No statistically significant changes were induced in endothelial cells in culture following exposure to serum from mice treated with MWCNT. A non-significant trend toward a decrease in cytokine gene expression in both young and old groups was observed for IL-6. Data assessed using 2-way ANOVA. $n = 5–6$ per group. Data presented are means ± SEM.
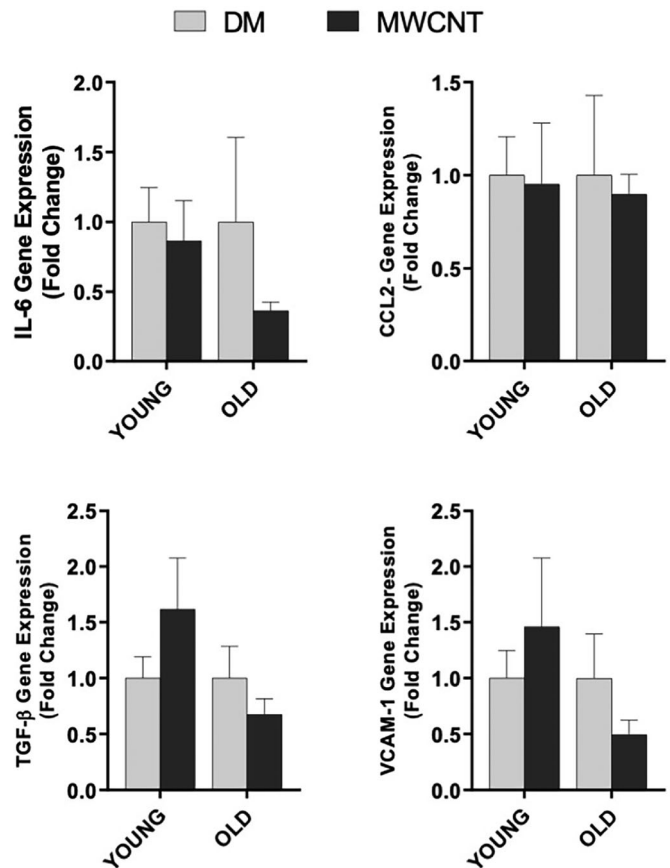

Figure 6. Serum Cumulative Inflammatory Potential (SCIP) assessment of serum from ApoE$^{-/-}$ female mice exposed to MWCNT. Mouse cerebrovascular endothelial cells (mCEC) were treated with serum from old and young dispersion media (DM) and MWCNT. Inflammatory gene expression changes were assessed via qPCR. No statistically significant changes were induced in endothelial cells in culture following exposure to serum from mice treated with MWCNT. Data assessed using 2-way ANOVA. $n = 5–6$ per group. Data presented are means ± SEM.

Apart from converse responses were seen in young DM and young MWCNT-exposed C57BL/6 mice, no other indicators of effect were seen. However, the NAD$^+$ precursor nicotinic acid adenine dinucleotide (NaAD) was strikingly similar to NAD$^+$ levels for all conditions, implying NaAD and the tryptophan pathway as the preferred cerebellar pathway for NAD$^+$ production. No statistical differences were observed in the NaAD precursor, nicotinic acid mononucleotide (NaMN), and the ATP consumption at this conversion step would appear to be rate-limiting for NaAD production. In turn, this would limit the production of NAD$^+$, as the NMN precursor was unchanged by exposure and age.

Discussion

In the present study, we assessed the lung inflammatory and neurometabolomic consequences of nanomaterial exposure in a susceptible model. We evaluated the role of age as a mitigating factor in MWCNT exposure-induced pulmonary and systemic outcomes in the hyperlipidemic ApoE$^{-/-}$ female mouse model. We demonstrated age-independent pulmonary inflammatory modulation in which the ApoE-null model of hypercholesterolemia played a significant role in exacerbating cellular responses to exposure. Additionally, we showed, as expected from previous studies, the robust neutrophil influx was induced in both ApoE$^{-/-}$ and C57BL/6 groups (assessed by BALF differential cell counts) by MWCNT exposure, although significantly more so in ApoE$^{-/-}$ (Shvedova et al. 2008; Han et al. 2015). A corresponding decrease in airway macrophages were observed in the ApoE$^{-/-}$ groups, but not in the C57BL/6, after MWCNT exposure. This differential expression between macrophages and neutrophils in ApoE$^{-/-}$ has been previously reported with carbon black, carbon nanotubes, and quantum dots (Jacobsen et al. 2009; Cao et al. 2014). Decreased macrophage function has also been reported with age and likely reflects an acceleration of particle clearance and influences the recruitment of inflammatory cells to sites of exposure. Additionally, persistent neutrophil presence in both local lung environment and systemic circulation is facilitated by age-related loss of clearance efficiency with concurrent increases in ROS production (Wang et al. 2010). The natural increase of BALF neutrophils with age is well documented (Meyer, 2001), although not observed in our study, as both old and young animals of both strains
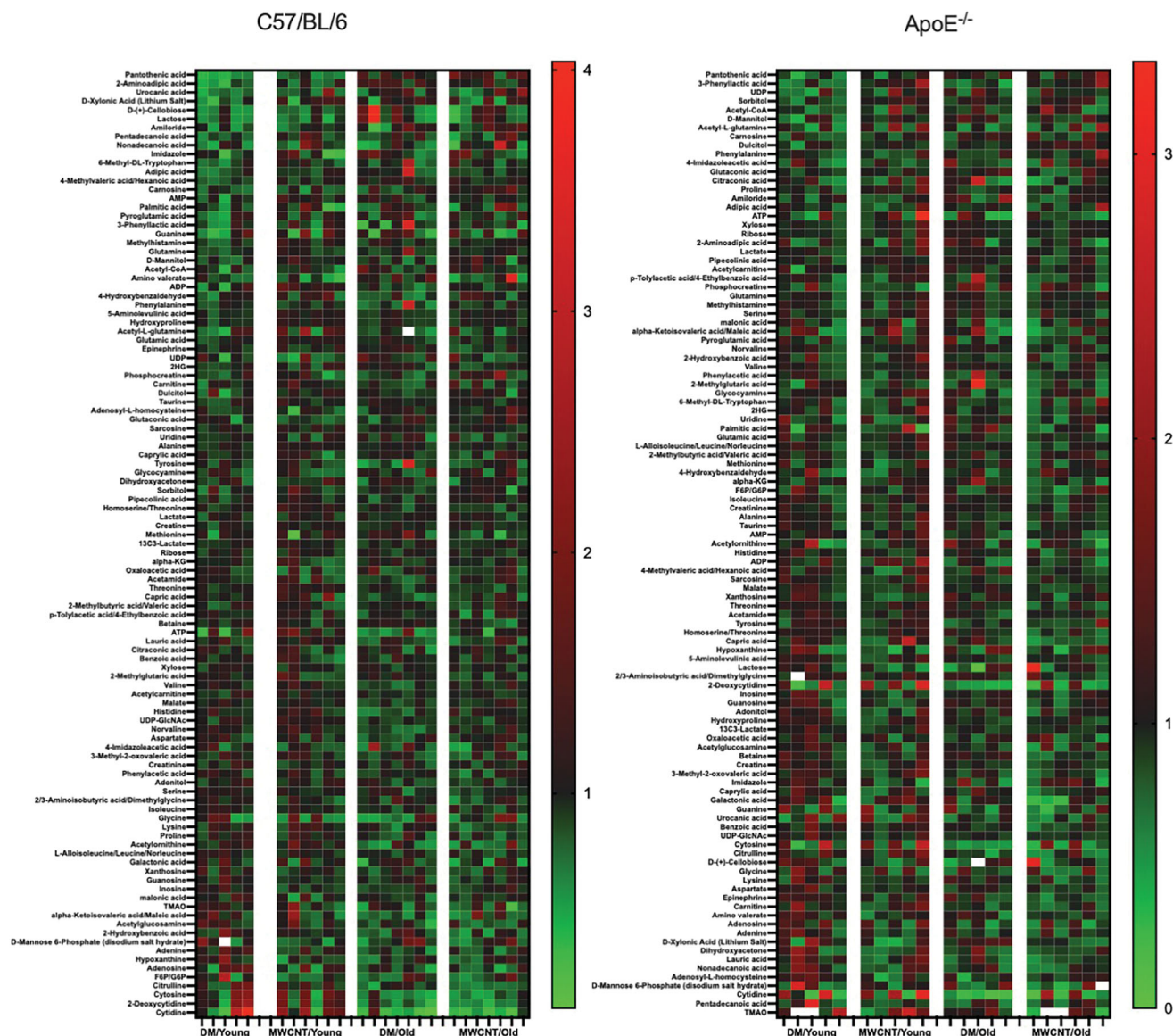
Figure 7. Heat map representation of cerebellar metabolomics of MWCNT-exposed C57BL/6 and APOE$^{-/-}$ female mice. Untargeted analysis of all metabolites assessed. $n = 5–7$ per group. Data presented are means ± SEM.
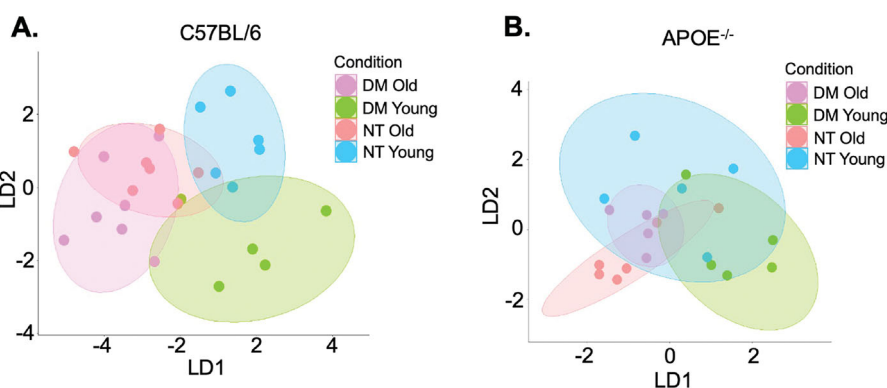

Figure 8. (A, B) Cerebellar metabolomics of MWCNT exposed C57BL/6 and APOE$^{-/-}$ female mice. C57BL/6 (left) and APOE$^{-/-}$ (right) linear discriminate analyses. C57BL/6 (left) and APOE (right) linear discriminate analyses. C57BL/6 accuracy was estimated at 80% by machine learning and 92% of variance was explained in the dimensions shown (LD1 $= 62.09\%$, LD2 $= 29.67\%$, LD3 $= 8.24\%$). ApoE was subjected to the same analysis. However, the amount of colinear variables deemed the accuracy at 66% by machine learning, with 79% of variance explained in the first two dimensions (LD1 $= 51.36\%$, LD2 $= 28.55\%$, LD3 $= 20.9\%$).
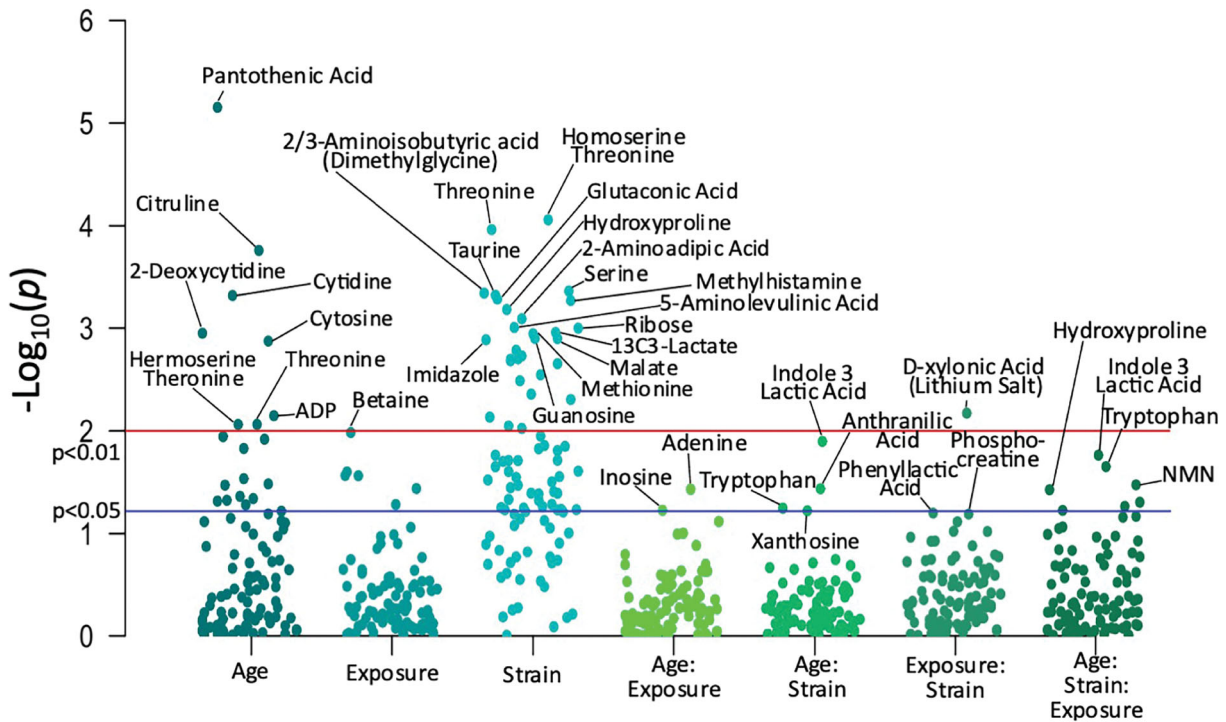
Figure 9. Manhattan plot of cerebellar metabolomics of MWCNT exposed C57BL/6 and APOE$^{-/-}$ female mice. 3-way ANOVA compared the influence of Age, MWCNT exposure, and Strain on the cerebellar metabolome. $n = 5–7$ per group. Data presented are means ± SEM.
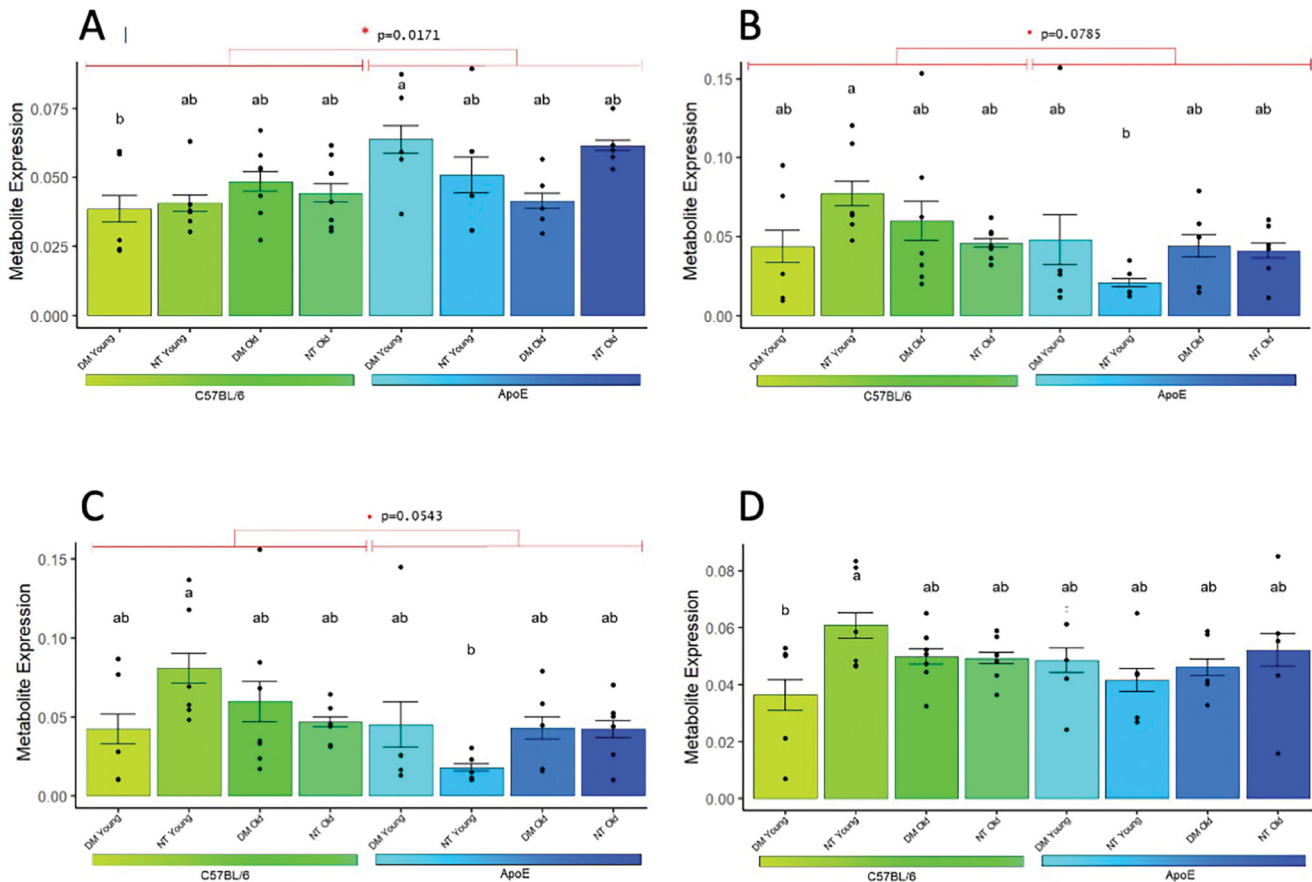

Figure 10. Cerebellar NAD$^+$ and related metabolites MWCNT exposed C57BL/6 and APOE$^{-/-}$ female mice. Targeted analysis revealed MWCNT exposure, age, and strain-related changes to NAD$^+$ and several related metabolites. $n = 5–7$ per group. Data presented are means ± SEM. Adenosine diphosphate (ADP); Adenosine triphosphate (ATP); Nicotinamide adenine dinucleotide (NAD); Nicotinamide riboside (NR); nicotinamide mononucleotide (NMN); nicotinamide (NAM); nicotinic acid mononucleotide (NaMN); nicotinic acid adenine dinucleotide (NaAD). NMN (A) and NaAD (B) are precursors to NAD+ (C). ADP Ribose (D) can be made from NAD$^+$ during times of DNA damage.

exhibited MWCNT exposure-induced increases independent of age. The expected adjuvant role of MWCNT in increasing neutrophil infiltration in aging animals was not observed in either C57BL/6 or ApoE$^{-/-}$ animals. In contrast to our findings in ozone-exposed animals (Tyler et al. 2018), C57BL/6 mice showed no significant changes in lung macrophages, although a non-significant trend toward overall lower macrophage presence was observed in older animals.

ApoE deficiency also exacerbated MWCNT-induced lung injury, as indicated by BALF protein, potentially due to enhanced pulmonary endothelial permeability (Yamashita et al. 2014) in older mice, an effect not seen in C57BL/6 mice. Increased vascular permeability with age is a common phenomenon resulting from vascular wall remodeling, barrier integrity changes, and general age-related functional decline in endothelial function (Krouwer et al. 2012). Previous studies of MWCNT exposure in ApoE$^{-/-}$ mice also demonstrated increased BALF total protein with various particulate and nanomaterial exposures (Han et al. 2015). Long et al. showed that oxidative stress played a significant role in altering human endothelial cell permeability *in vitro* with MWCNT exposure increased ROS (Long et al. 2017) and lipid accumulation in THP-1 macrophages cell lines (Long et al. 2019). Although not assessed here, we also previously reported a corresponding increase in the cellular damage marker, lactate dehydrogenase, as an accompanying feature of MWCNT and other particulate exposures (Campen et al. 2014; Aragon, Erdely, et al. 2016; Tyler et al. 2016). These findings are important from a clinical perspective, since increased vascular permeability is common in aging and associated with adverse cardiovascular and neurological outcomes.

We have previously demonstrated significant serum peptide compositional changes following MWCNT exposure, which appear to be pulmonary-derived and impair blood–brain barrier permeability with accompanying neuroinflammatory activation (Aragon et al. 2017; Mostovenko et al. 2019). Such a transfer of bioactivity may be facilitated by cytotoxicity induced by exposure as a result of increased oxidative stress resulting in the impaired alveolar air-blood barrier as has been shown in prior studies using PM and nanomaterials (Caraballo et al. 2011; Andreau et al. 2012; Porter et al. 2013; Byun et al. 2019; Liu et al. 2019; Sokolowska et al. 2019). The reduction in blood–brain barrier has been shown with other inhaled toxicants and is a likely pathway by which pulmonary toxicity can contribute to acute and long-term neurological outcomes (Mumaw et al. 2016; Aragon et al. 2017; Tyler et al. 2018). Blood–brain barrier deficits are apparent in numerous neurological diseases, initiate neuroinflammatory outcomes, and are conjectured to be an essential player in the pathogenesis of aging-related neurodegenerative diseases (Heneka et al. 2015; Nation et al. 2019). Additionally, Stapleton et al. reported serum albumin in BALF following MWCNT exposure (Stapleton et al. 2012), which introduction into the airways might exacerbate inflammatory responses leading to further dysregulation of the airway–blood barrier. ApoE$^{-/-}$ mice have been shown to be susceptible to pulmonary endothelial damage directly related to increased oxidized lipids (Yamashita et al. 2014). Higher baseline cholesterol levels in ApoE$^{-/-}$ (Lo Sasso et al. 2016), along with toxicity from MWCNT exposure compounds oxidative stress appeared to promote endothelial and epithelial dysfunction and subsequent systemic inflammatory activation by pulmonary derived bioactives.

Pro-inflammatory mediators such as TNF-α, TGF-β and IFNγ are known to alter endothelial homeostasis through disrupted endothelial cell proliferation, increased permeability, and altered endothelial cell connections/communication with the extracellular matrix (Seynhaeve et al. 2006). We assessed the levels of chemokines and cytokines in BALF of ApoE$^{-/-}$ and C57BL/6 mice exposed to MWCNT in this study. Similar patterns of expression were observed between C57BL/6 and ApoE$^{-/-}$ animals, with exposure increasing most cytokines assessed. C57BL/6 showed the greatest age-related expression changes in cytokine expression with IL-1β, IL-6, MCP-1 being increased in old animals, while CXCL1 and CXCL10 were decreased. Only CXCL1, CXCL10 (mimicking the decrease in the controls), and IFNγshowed age-related effects in ApoE$^{-/-}$. Given the high levels of CCL2, a monocyte/macrophage attractant, one might expect a corresponding increase in BALF macrophages but this was not the case in our acute study. The role of CCL2 in neutrophil recruitment is much debated; however, studies have shown that neutrophil recruitment and function at sites of bacterial infection in the lung was impaired in CCL2$^{-/-}$ animals (Balamayooran et al. 2011; Jin et al. 2018). Despite similar neutrophil counts in the BALF of both age groups and strains, CCL2 was more significantly elevated in old C57BL/6 mice compared to young animals, while levels were not different between ApoE$^{-/-}$ age groups. Elevated CCL2 levels also persist in aged ApoE$^{-/-}$ when larger doses and longer experimental time points are employed (Vesterdal et al. 2010). Decreases were also observed in the expression levels of CXCL1 and CXCL10 in the aged animals in both the C57BL/6 and ApoE$^{-/-}$ groups. CXCL1, which plays a key role in neutrophil recruitment and activation, was surprising given the increase in neutrophils observed in these groups. CXCL1 exists as both monomers and dimers, with both the monomer and dimer activating the CXCR2 receptors in neutrophils (Sawant et al. 2016). CXCL10 is secreted in response to IFNγ signaling from and so the observed decrease in ApoE$^{-/-}$ is understandable given the significant decrease in IFNγ levels. The substantial decrease in CXCL10 response to MWCNT in C57BL/6 aged animals is harder to explain and the implications are unclear.

Surprisingly, the bioactivity of serum from exposed female mice did not induce an inflammatory response in endothelial cells grown in culture in any of the groups assessed. This is in stark contrast to several previous studies showing increased inflammatory activation induced by MWCNT-exposed serum, when compared to serum from unexposed animals (Aragon, Erdely, et al. 2016; Aragon, Chrobak, et al. 2016, 2017; Mostovenko et al. 2019, 2021). We conclude that batches of primary endothelial cells may

exhibit different sensitivity, contributing uncertainty to such approaches. Alternatively, as most previous works were conducted in male mice, there is a possibility that female mouse serum is more protective of inflammatory alteration. While we have previously considered using such approaches as more broadly applicable clinical assessments of vascular risk, the present findings represent an important caveat that standardization of this *ex vivo/in vitro* methods may be more complicated than previously thought.

Further assessment of the systemic consequences of pulmonary exposure to MWCNT centered on neurometabolic changes. The brain has high energy demands that must be maintained for optimal function. As we age, the loss in metabolic capacity often foreshadows cognitive impairments (Wyss-Coray 2016). The aging neuron is vulnerable to reduced metabolic capacity, highlighted as a loss of nicotinamide adenine dinucleotide (NAD+) concentrations, increased AMP/ATP ratio, and purine and pyrimidine accumulation (Ivanisevic et al. 2016). This reduction in bioenergetics adversely impacts DNA repair mechanisms which appear central to a downward spiral of cellular functionality (Fang et al. 2016; Hou et al. 2018; Nacarelli et al. 2019). Mice in the present study were not truly of 'advanced age,' but at 15 months (approximately mid-40s in humans), there were still substantial metabolic differences compared to 2-month-old mice (approximately 20 years old in humans). Cerebellar metabolomic responses to MWCNT were modest, but statistically significant effects still highlight the systemic ramifications of pulmonary particulate exposures. Holistically, the aged mice exhibited a less robust response to MWCNT than young mice, based on the principal component analysis. This was most notable for NAD+, interestingly, with young mice displaying an increase in NAD + levels, but this response was dampened in older mice and in the ApoE$^{-/-}$ mice. Several metabolites were altered by aging that has been previously identified as aging-related metabolites in the cerebellum, including pantothenic acid, citrulline, adenosine, and carnosine. However, MWCNT alone altered only a few (World Health Organization 2018) published factors that are altered in the cerebellum by aging, including pantothenic acid and betaine (Ding et al. 2021). MWCNT interactions with aging, strain, and both were also apparent, suggesting that complex pathways and responses may be involved in the linkage between lung inflammation and neurometabolic changes. Future studies should examine these metabolomic outcomes across a wider range of response times, as well as in mice in the 18–24 month range. The 15-month-old mouse is more of a model of middle age in humans, but as such may model a perimenopausal period. The impact of MWCNT exposure in perimenopausal women, whose hormonal changes may leave them already susceptible to cognitive impairments (Henderson and Brinton 2010; Vega et al. 2016; Devi 2018), should be considered in future studies.

The most obvious caveat to the straightforward interpretation of these studies is the difference in body weight between the young (∼20 g) and old (∼35 g) mice, for both strains. This difference in body weight means that older mice effectively received a reduced relative dose of MWCNT. In terms of those cytokines or other measures that appeared reduced in comparing the old versus young mice, for example, CXCL1 and CXCL10, this diminution of response may mostly relate to the lower relative dose of MWCNT in older (larger) mice. However, this consideration of body weight amplifies the impact of those markers clearly increased in older mice, such as the IL-6, IL1β, and MCP-1 responses in C57BL/6 mice, and overall total protein levels in lavage from both strains.

Here we reported on the inflammatory potential of short-term MWCNT exposure in an aging WT and ApoE$^{-/-}$ mouse model. ApoE deficiency resulted in more robust pulmonary inflammatory cell recruitment and increased lung damage. While the modestly advanced age of 15 months did not seem to play a major role in the inflammatory activation, the extent of protein leakage resulting from exposure was significantly worse in older mice, indicating a risk of more adverse and possibly prolonged effects in older populations. Additionally, while cerebellar metabolic changes indicated a modest CNS response to the MWCNT exposure, aging seemed to diminish responsiveness.

Disclosure statement

Funding

ORCID

Katherine Zychowski http://orcid.org/0000-0002-5751-2897
Matthew J. Campen http://orcid.org/0000-0002-2292-5050

References

Achariyar TM, Li B, Peng W, Verghese PB, Shi Y, McConnell E, Benraiss A, Kasper T, Song W, Takano T, et al. 2016. Glymphatic distribution of CSF-derived apoE into brain is isoform specific and suppressed during sleep deprivation. Mol Neurodegener. 11(1):74.

Andreau K, Leroux M, Bouharrour A. 2012. Health and cellular impacts of air pollutants: from cytoprotection to cytotoxicity. Biochem Res Int. 2012:493894.

Aragon M, Erdely A, Bishop L, Salmen R, Weaver J, Liu J, Hall P, Eye T, Kodali V, Zeidler-Erdely P, et al. 2016. MMP-9-dependent serum-borne bioactivity caused by multiwalled carbon nanotube exposure induces vascular dysfunction via the CD36 scavenger receptor. Toxicol Sci. 150(2):488–498.

Aragon MJ, Chrobak I, Brower J, Roldan L, Fredenburgh LE, McDonald JD, Campen MJ. 2016. Inflammatory and vasoactive effects of serum following inhalation of varied complex mixtures. Cardiovasc Toxicol. 16(2):163–171.

Aragon MJ, Topper L, Tyler CR, Sanchez B, Zychowski K, Young T, Herbert G, Hall P, Erdely A, Eye T, et al. 2017. Serum-borne bio-activity caused by pulmonary multiwalled carbon nanotubes induces neuroinflammation via blood-brain barrier impairment. Proc Natl Acad Sci USA. 114(10):E1968–E1976.

Balamayooran G, Batra S, Balamayooran T, Cai S, Jeyaseelan S. 2011. Monocyte chemoattractant protein 1 regulates pulmonary host defense via neutrophil recruitment during *Escherichia coli* infection. Infect Immun. 79(7):2567–2577.

Bektas A, Schurman SH, Sen R, Ferrucci L. 2018. Aging, inflammation and the environment. Exp Gerontol. 105:10–18. Epub 2017/12/25. PubMed PMID: 29275161; PMCID: PMC5909704.

Bratic A, Larsson NG. 2013. The role of mitochondria in aging. J Clin Invest. 123(3):951–957.

Brook RD, Rajagopalan S, Pope CA, 3rd, Brook JR, Bhatnagar A, Diez-Roux AV, Holguin F, Hong Y, Luepker RV, Mittleman MA, et al. 2010. Particulate matter air pollution and cardiovascular disease: an update to the scientific statement from the American Heart Association. Circulation. 121(21):2331–2378.

Byun J, Song B, Lee K, Kim B, Hwang HW, Ok MR, Jeon H, Lee K, Baek SK, Kim SH, et al. 2019. Identification of urban particulate matter-induced disruption of human respiratory mucosa integrity using whole transcriptome analysis and organ-on-a chip. J Biol Eng. 13:88.

Campen M, Robertson S, Lund A, Lucero J, McDonald J. 2014. Engine exhaust particulate and gas phase contributions to vascular toxicity. Inhal Toxicol. 26(6):353–360.

Cao Y, Jacobsen NR, Danielsen PH, Lenz AG, Stoeger T, Loft S, Wallin H, Roursgaard M, Mikkelsen L, Moller P. 2014. Vascular effects of multiwalled carbon nanotubes in dyslipidemic ApoE$^{-/-}$ mice and cultured endothelial cells. Toxicol Sci. 138(1):104–116.

Caraballo JC, Yshii C, Westphal W, Moninger T, Comellas AP. 2011. Ambient particulate matter affects occludin distribution and increases alveolar transepithelial electrical conductance. Respirology. 16(2):340–349.

Carroll PA, Diolaiti D, McFerrin L, Gu H, Djukovic D, Du J, Cheng PF, Anderson S, Ulrich M, Hurley JB, et al. 2015. Deregulated Myc requires MondoA/Mlx for metabolic reprogramming and tumorigenesis. Cancer Cell. 27(2):271–285.

Cung H, Aragon MJ, Zychowski K, Anderson JR, Nawarskas J, Roldan C, Sood A, Qualls C, Campen MJ. 2015. Characterization of a novel endothelial biosensor assay reveals increased cumulative serum inflammatory potential in stabilized coronary artery disease patients. J Transl Med. 13:99.

Devi G. 2018. Menopause-related cognitive impairment. Obstet Gynecol. 132(6):1325–1327.

Ding J, Ji J, Rabow Z, Shen T, Folz J, Brydges CR, Fan S, Lu X, Mehta S, Showalter MR, et al. 2021. A metabolome atlas of the aging mouse brain. Nat Commun. 12(1):6021.

Dockery DW, Pope CA, 3rd, Kanner RE, Martin Villegas G, Schwartz J. 1999. Daily changes in oxygen saturation and pulse rate associated with particulate air pollution and barometric pressure. Res Rep Health Eff Inst. 83:1–19.

Eghlimi R, Shi XJ, Hrovat J, Xi BW, Gu HW. 2020. Triple negative breast cancer detection using LC-MS/MS lipidomic profiling. J Proteome Res. 19(6):2367–2378.

Erdely A, Dahm M, Chen BT, Zeidler-Erdely PC, Fernback JE, Birch ME, Evans DE, Kashon ML, Deddens JA, Hulderman T, et al. 2013. Carbon nanotube dosimetry: from workplace exposure assessment to inhalation toxicology. Part Fibre Toxicol. 10(1):53.

Fang EF, Kassahun H, Croteau DL, Scheibye-Knudsen M, Marosi K, Lu H, Shamanna RA, Kalyanasundaram S, Bollineni RC, Wilson MA, et al. 2016. NAD + replenishment improves lifespan and healthspan in ataxia telangiectasia models via mitophagy and DNA repair. Cell Metab. 24(4):566–581.

Fraser K, Kodali V, Yanamala N, Birch ME, Cena L, Casuccio G, Bunker K, Lersch TL, Evans DE, Stefaniak A, et al. 2020. Physicochemical characterization and genotoxicity of the broad class of carbon nanotubes and nanofibers used or produced in U.S. facilities. Part Fibre Toxicol. 17(1):62.

Grande G, Ljungman PLS, Eneroth K, Bellander T, Rizzuto D. 2020. Association between cardiovascular disease and long-term exposure to air pollution with the risk of dementia. JAMA Neurol. 77(7): 801–809.

Gu H, Carroll PA, Du J, Zhu J, Neto FC, Eisenman RN, Raftery D. 2016. Quantitative method to investigate the balance between metabolism and proteome biomass: starting from glycine. Angew Chem Int Ed Engl. 55(50):15646–15650.

Gu H, Zhang P, Zhu J, Raftery D. 2015. Globally optimized targeted mass spectrometry: reliable metabolomics analysis with broad coverage. Anal Chem. 87(24):12355–12362.

Han SG, Howatt D, Daugherty A, Gairola G. 2015. Pulmonary and atherogenic effects of multi-walled carbon nanotubes (MWCNT) in apolipoprotein-E-deficient mice. J Toxicol Environ Health A. 78(4): 244–253.

He J, Zhu Z, Bundy JD, Dorans KS, Chen J, Hamm LL. 2021. Trends in cardiovascular risk factors in US adults by race and ethnicity and socioeconomic status, 1999-2018. JAMA. 326(13):1286–1298.

Henderson VW, Brinton RD. 2010. Menopause and mitochondria: windows into estrogen effects on Alzheimer's disease risk and therapy. Prog Brain Res. 182:77–96.

Heneka MT, Carson MJ, El Khoury J, Landreth GE, Brosseron F, Feinstein DL, Jacobs AH, Wyss-Coray T, Vitorica J, Ransohoff RM, et al. 2015. Neuroinflammation in Alzheimer's disease. Lancet Neurol. 14(4):388–405.

Hou Y, Lautrup S, Cordonnier S, Wang Y, Croteau DL, Zavala E, Zhang Y, Moritoh K, O'Connell JF, Baptiste BA, et al. 2018. NAD + supplementation normalizes key Alzheimer's features and DNA damage responses in a new AD mouse model with introduced DNA repair deficiency. Proc Natl Acad Sci USA. 115(8): E1876–E1885.

Ivanisevic J, Stauch KL, Petrascheck M, Benton HP, Epstein AA, Fang M, Gorantla S, Tran M, Hoang L, Kurczy ME, et al. 2016. Metabolic drift in the aging brain. Aging. 8(5):1000–1020.

Jacobsen NR, Moller P, Jensen KA, Vogel U, Ladefoged O, Loft S, Wallin H. 2009. Lung inflammation and genotoxicity following pulmonary exposure to nanoparticles in ApoE-/- mice. Part Fibre Toxicol. 6:2.

Jasbi P, Mitchell NM, Shi XJ, Grys TE, Wei YP, Liu L, Lake DF, Gu HW. 2019. Coccidioidomycosis detection using targeted plasma and urine metabolic profiling. J Proteome Res. 18(7):2791–2802.

Jin L, Ghimire L, Paudel S, Cai S, Rangasamy T, Jeyaseelan S. 2018. MCP-1 plays a critical role in neutrophil function and pyroptosis during carbapenemf-resistant *Klebsiella pneumoniae*. J Immunol. 200(1):46.17.

Krouwer VJ, Hekking LH, Langelaar-Makkinje M, Regan-Klapisz E, Post JA. 2012. Endothelial cell senescence is associated with disrupted cell-cell junctions and increased monolayer permeability. Vasc Cell. 4(1):12.

Kulminski AM, Barochia AV, Loika Y, Raghavachari N, Arbeev KG, Wojczynski MK, Thyagarajan B, Vardarajan BN, Christensen K, Yashin AI, et al. 2018. The APOE ε4 allele is associated with a reduction in FEV1/FVC in women: a cross-sectional analysis of the long life family study. PLoS One. 13(11):e0206873.

Leng F, Edison P. 2021. Neuroinflammation and microglial activation in Alzheimer disease: where do we go from here? Nat Rev Neurol. 17(3):157–172.

Liu CC, Liu CC, Kanekiyo T, Xu H, Bu G. 2013. Apolipoprotein E and Alzheimer disease: risk, mechanisms and therapy. Nat Rev Neurol. 9(2):106–118.

Liu J, Chen X, Dou M, He H, Ju M, Ji S, Zhou J, Chen C, Zhang D, Miao C, et al. 2019. Particulate matter disrupts airway epithelial barrier via oxidative stress to promote *Pseudomonas aeruginosa* infection. J Thorac Dis. 11(6):2617–2627.

Lo Sasso G, Schlage WK, Boue S, Veljkovic E, Peitsch MC, Hoeng J. 2016. The Apoe(-/-) mouse model: a suitable model to study cardiovascular and respiratory diseases in the context of cigarette smoke exposure and harm reduction. J Transl Med. 14(1):146.

Long J, Ma W, Yu Z, Liu H, Cao Y. 2019. Multi-walled carbon nanotubes (MWCNTs) promoted lipid accumulation in THP-1

macrophages through modulation of endoplasmic reticulum (ER) stress. Nanotoxicology. 13(7):938.

Long J, Xiao Y, Liu L, Cao Y. 2017. The adverse vascular effects of multi-walled carbon nanotubes (MWCNTs) to human vein endothelial cells (HUVECs) in vitro: role of length of MWCNTs. J Nanobiotechnology. 15(1):80.

Meyer KC. 2001. The role of immunity in susceptibility to respiratory infection in the aging lung. Respir Physiol. 128(1):23–31.

Mostovenko E, Saunders S, Muldoon PP, Bishop L, Campen MJ, Erdely A, Ottens AK. 2021. Carbon nanotube exposure triggers a cerebral peptidomic response: barrier compromise, neuroinflammation, and a hyperexcited state. Toxicol Sci. 182(1):107–119.

Mostovenko E, Young T, Muldoon PP, Bishop L, Canal CG, Vucetic A, Zeidler-Erdely PC, Erdely A, Campen MJ, Ottens AK. 2019. Nanoparticle exposure driven circulating bioactive peptidome causes systemic inflammation and vascular dysfunction. Part Fibre Toxicol. 16(1):20.

Mulder M. 2009. Sterols in the central nervous system. Curr Opin Clin Nutr Metab Care. 12(2):152–158.

Mumaw CL, Levesque S, McGraw C, Robertson S, Lucas S, Stafflinger JE, Campen MJ, Hall P, Norenberg JP, Anderson T, et al. 2016. Microglial priming through the lung-brain axis: the role of air pollution-induced circulating factors. FASEB J. 30(5):1880–1891.

Nacarelli T, Lau L, Fukumoto T, Zundell J, Fatkhutdinov N, Wu S, Aird KM, Iwasaki O, Kossenkov AV, Schultz D, et al. 2019. NAD + metabolism governs the proinflammatory senescence-associated secretome. Nat Cell Biol. 21(3):397–407.

Nation DA, Sweeney MD, Montagne A, Sagare AP, D'Orazio LM, Pachicano M, Sepehrband F, Nelson AR, Buennagel DP, Harrington MG, et al. 2019. Blood-brain barrier breakdown is an early biomarker of human cognitive dysfunction. Nat Med. 25(2):270–276.

Poole JA, Romberger DJ, Wyatt TA, Staab E, VanDeGraaff J, Thiele GM, Dusad A, Klassen LW, Duryee MJ, Mikuls TR, et al. 2015. Age impacts pulmonary inflammation and systemic bone response to inhaled organic dust exposure. J Toxicol Environ Health A. 78(19): 1201–1216.

Pope CA, 3rd, Burnett RT, Thurston GD, Thun MJ, Calle EE, Krewski D, Godleski JJ. 2004. Cardiovascular mortality and long-term exposure to particulate air pollution: epidemiological evidence of general pathophysiological pathways of disease. Circulation. 109(1):71–77.

Pope CA, 3rd, Ezzati M, Dockery DW. 2009. Fine-particulate air pollution and life expectancy in the United States. N Engl J Med. 360(4): 376–386.

Porter DW, Hubbs AF, Chen BT, McKinney W, Mercer RR, Wolfarth MG, Battelli L, Wu N, Sriram K, Leonard S, et al. 2013. Acute pulmonary dose-responses to inhaled multi-walled carbon nanotubes. Nanotoxicology. 7(7):1179–1194.

Porter DW, Hubbs AF, Mercer RR, Wu N, Wolfarth MG, Sriram K, Leonard S, Battelli L, Schwegler-Berry D, Friend S, et al. 2010. Mouse pulmonary dose- and time course-responses induced by exposure to multi-walled carbon nanotubes. Toxicology. 269(2–3): 136–147.

Sawant KV, Poluri KM, Dutta AK, Sepuru KM, Troshkina A, Garofalo RP, Rajarathnam K. 2016. Chemokine CXCL1 mediated neutrophil recruitment: role of glycosaminoglycan interactions. Sci Rep. 6(1): 33123.

Schubauer-Berigan MK, Dahm MM, Erdely A, Beard JD, Eileen Birch M, Evans DE, Fernback JE, Mercer RR, Bertke SJ, Eye T, et al. 2018. Association of pulmonary, cardiovascular, and hematologic metrics with carbon nanotube and nanofiber exposure among U.S. workers: a cross-sectional study. Part Fibre Toxicol. 15(1):22.

Seynhaeve ALB, Vermeulen CE, Eggermont AMM, ten Hagen TLM. 2006. Cytokines and vascular permeability: an in vitro study on human endothelial cells in relation to tumor necrosis factor-alpha-primed peripheral blood mononuclear cells. CBB. 44(1):157–169.

Shi XJ, Wang S, Jasbi P, Turner C, Hrovat J, Wei YP, Liu JP, Gu HW. 2019. Database-assisted globally optimized targeted mass spectrometry (dGOT-MS): broad and reliable metabolomics analysis with enhanced identification. Anal Chem. 91(21):13737–13745.

Shvedova AA, Kisin E, Murray AR, Johnson VJ, Gorelik O, Arepalli S, Hubbs AF, Mercer RR, Keohavong P, Sussman N, et al. 2008. Inhalation vs. aspiration of single-walled carbon nanotubes in C57BL/6 mice: inflammation, fibrosis, oxidative stress, and mutagenesis. Am J Physiol Lung Cell Mol Physiol. 295(4):L552–L565.

Smith TR, Bhatnagar A. 2018. Enviromics: understanding aging. Aging. 11(1):9–10.

Sokolowska M, Quesniaux VFJ, Akdis CA, Chung KF, Ryffel B, Togbe D. 2019. Acute respiratory barrier disruption by ozone exposure in mice. Front Immunol. 10:2169.

Stapleton PA, Minarchick VC, Cumpston AM, McKinney W, Chen BT, Sager TM, Frazer DG, Mercer RR, Scabilloni J, Andrew ME, et al. 2012. Impairment of coronary arteriolar endothelium-dependent dilation after multi-walled carbon nanotube inhalation: a time-course study. Int J Mol Sci. 13(11):13781–13803.

Tyler CR, Noor S, Young TL, Rivero V, Sanchez B, Lucas S, Caldwell KK, Milligan ED, Campen MJ. 2018. Aging exacerbates neuroinflammatory outcomes induced by acute ozone exposure. Toxicol Sci. 163(1):123–139.

Tyler CR, Zychowski KE, Sanchez BN, Rivero V, Lucas S, Herbert G, Liu J, Irshad H, McDonald JD, Bleske BE, et al. 2016. Surface area-dependence of gas-particle interactions influences pulmonary and neuroinflammatory outcomes. Part Fibre Toxicol. 13(1):64.

Vega JN, Zurkovsky L, Albert K, Melo A, Boyd B, Dumas J, Woodward N, McDonald BC, Saykin AJ, Park JH, et al. 2016. Altered brain connectivity in early postmenopausal women with subjective cognitive impairment. Front Neurosci. 10:433.

Vesterdal LK, Folkmann JK, Jacobsen NR, Sheykhzade M, Wallin H, Loft S, Moller P. 2010. Pulmonary exposure to carbon black nanoparticles and vascular effects. Part Fibre Toxicol. 7:33.

Wagner KH, Cameron-Smith D, Wessner B, Franzke B. 2016. Biomarkers of aging: from function to molecular biology. Nutrients. 8(6):338.

Wang L, Green FH, Smiley-Jewell SM, Pinkerton KE. 2010. Susceptibility of the aging lung to environmental injury. Semin Respir Crit Care Med. 31(5):539–553.

World Health Organization. 2018. Fact sheet: Ambient (outdoor) air pollution Geneva (Switzerland): WHO.

Wyss-Coray T. 2016. Ageing, neurodegeneration and brain rejuvenation. Nature. 539(7628):180–186.

Yamashita CM, Fessler MB, Vasanthamohan L, Lac J, Madenspacher J, McCaig L, Yao L, Wang L, Puntorieri V, Mehta S, et al. 2014. Apolipoprotein E-deficient mice are susceptible to the development of acute lung injury. Respiration. 87(5):416–427.

Yao X, Gordon EM, Figueroa DM, Barochia AV, Levine SJ. 2016. Emerging roles of apolipoprotein E and apolipoprotein A-I in the pathogenesis and treatment of lung disease. Am J Respir Cell Mol Biol. 55(2):159–169.

Yin Y, Wang Z. 2018. ApoE and neurodegenerative diseases in aging. Adv Exp Med Biol. 1086:77–92.

Zhang SH, Reddick RL, Piedrahita JA, Maeda N. 1992. Spontaneous hypercholesterolemia and arterial lesions in mice lacking apolipoprotein E. Science. 258(5081):468–471.

Zhao N, Liu CC, Qiao W, Bu G. 2018. Apolipoprotein E, receptors, and modulation of Alzheimer's disease. Biol Psychiatry. 83(4): 347–357.

Zychowski KE, Sanchez B, Pedrosa RP, Lorenzi-Filho G, Drager LF, Polotsky VY, Campen MJ. 2016. Serum from obstructive sleep apnea patients induces inflammatory responses in coronary artery endothelial cells. Atherosclerosis. 254:59–66.